

# Electromagnetically induced absorption and transparency due to resonant two-field excitation of quasidegenerate levels in Rb vapor

A. M. Akulshin,\* S. Barreiro, and A. Lezama

*Instituto de Física, Facultad de Ingeniería, Casilla de correo 30, 11000 Montevideo, Uruguay*

(Received 4 September 1997)

Positive and negative subnatural-width resonances (SNWR) were observed in the absorption and fluorescence of rubidium vapor under excitation by two copropagating optical waves with variable frequency offset. The two optical fields resonantly couple Zeeman sublevels, belonging to the same ground-state hyperfine level (GSHL), to an intermediate excited state. The SNWR present opposite signs depending on which GSHL participates in the interaction with the two optical waves. For both Rb isotopes an increase in the transparency with reduced fluorescence occurs for the lower GSHL while the absorption and fluorescence are increased for the upper GSHL. The influence of external magnetic field, polarization, and intensity of applied optical fields on the SNWR is examined. The narrowest observed resonance has a width of 10 kHz (full width at half maximum). The origin of the SNWR is discussed in terms of coherent processes involving ground-state Zeeman sublevels. [S1050-2947(98)06703-1]

PACS number(s): 42.50.Gy, 42.62.Fi, 32.70.Jz

## I. INTRODUCTION

The coherent superposition of atomic states induced by resonant radiation forms the base for a wealth of interesting phenomena in nonlinear laser spectroscopy. In most cases, the new phenomena are the consequence of quantum interference between dressed states [1–3]. Among these phenomena, coherent population trapping (CPT) [2–5], electromagnetically induced transparency (EIT) [6,7], enhancement of the refractive index without absorption [8], and lasing without inversion (LWI) [9] have received considerable attention in recent years. Different atomic three-level configurations,  $\Lambda$ -type,  $V$ -type, and cascade, were examined in relation to the above-mentioned effects.

Besides fundamental interest, these phenomena have promising applications. The suppression of absorption on resonant transitions can lead to large increases in the nonlinear susceptibilities [10]. Coherence induced between ground-state hyperfine levels was used for velocity selection in atomic fountains [11] and for subrecoil laser cooling [12]. The dispersive properties of an atomic intracavity medium in a dark state were used to stabilize the frequency difference between two laser diodes [13]. Also, the rapidly varying refractive index associated to EIT has been suggested as the base for a high precision magnetometer [14]. Recently EIT was used for isotope discrimination [15]. Narrow atomic absorption resonances and large values of the associated dispersion [16] are key elements of most if not all of these applications.

In spite of the large activity in the field, the spectral properties of coherently driven atomic media have not yet been studied exhaustively. Most investigations are based on simplified three-level models, while actual systems generally involve more complicated situations due to the magnetic struc-

ture of the concerned levels. For instance, EIT and CPT in alkaline-metal atoms in the folded ( $\Lambda$ -type) level configuration have been observed with both ground-state hyperfine levels participating in the process and with magnetic sublevels considered as degenerate [2–4,7,8,16]. Only in a few experiments concerned with cold atoms in optical traps was the interaction of several optical fields with the same ground-state hyperfine level (GSHL) considered [17–19].

The subject of this paper is the investigation of subnatural-width resonances (SNWR) induced by coherence among states belonging to the same atomic GSHL of alkaline-metal atoms. The SNWR were observed in the absorption and fluorescence of rubidium vapor illuminated by two mutually coherent copropagating optical waves that resonantly couple Zeeman sublevels belonging to the same GSHL to a common excited state.

Depending on the orientation of the external magnetic field and the polarization of the optical waves, the nearly degenerate atomic system can give rise to a wealth of different level configurations coupled by the optical fields. Some examples are shown in Fig. 1.

If the polarizations of the two incident fields relative to the magnetic field are different, for instance  $\sigma^+$  and  $\sigma^-$ , the energy-level structure may correspond to a  $\Lambda$  configuration [Fig. 1(a)] or to a more complex multiple coupled level combination [Fig. 1(b)]. It has been shown [5] that CPT can take place in such level configurations provided that the degeneracy of the excited state is smaller than or equal to the degeneracy of the ground state [ $(2F+1) \geq (2F'+1)$ ;  $F$  and  $F'$  are the total angular momentum of the ground and excited state, respectively]. In a  $\Lambda$  system, the minimum width of the absorption resonance obtained with two copropagating mutually coherent optical waves is given by  $\Gamma_{\min} = \gamma_1 + \gamma_2 + \gamma_c(1 - \omega_1/\omega_2)$ , where  $\gamma_1, \gamma_2$  are the relaxation rates of the lower levels and  $\omega_1, \omega_2$  are the optical frequencies of the two waves [1]. Consequently, for  $\omega_1 \cong \omega_2$  the resonance width approaches  $\Gamma_{\min} = (\gamma_1 + \gamma_2)$ . For atomic ground states, when collisions can be neglected,  $\gamma_{1,2}$  are very small com-

\*Permanent address: P. N. Lebedev Physics Institute, 117924 Moscow, Russia.

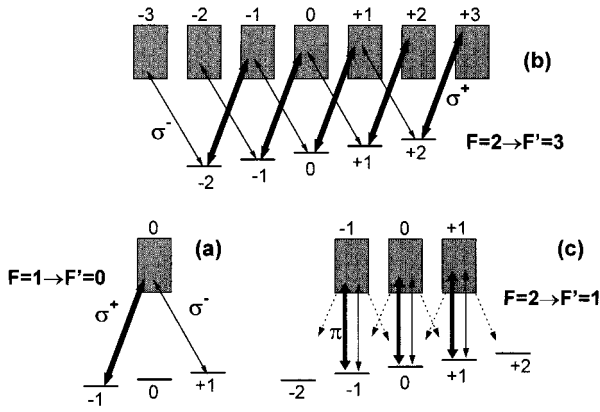


FIG. 1. Examples of energy-level configurations coupled by the pump and probe fields for different polarizations. The examples correspond to cycling transitions of  $^{87}\text{Rb}$  (a) and (b) and  $^{85}\text{Rb}$  (c). The dashed arrows represent spontaneous emission relaxation.

pared to the excited-state relaxation rate. In this case,  $\Gamma_{\min}$  is determined by the atomic transit time through the interaction region.

On the other hand, if the polarizations of the optical fields are the same (both  $\sigma^+$ ,  $\sigma^-$ , or  $\pi$ ), the level configuration can be thought of as a superposition of two-level systems only coupled to other states through spontaneous emission [Fig. 1(c)]. For two-level atoms, two mechanisms are responsible for the nonlinear resonances observed in absorption or fluorescence in a copropagating pump-probe experiment. The first mechanism related to population redistribution gives rise to the familiar saturated absorption resonance of width  $\Gamma = (\gamma_e + \gamma_g)$ , where  $\gamma_e$  and  $\gamma_g$  are the relaxation rates of the excited and ground states, respectively. The second more subtle mechanism involves the coherence among the atomic states. As for CPT in a  $\Lambda$  system, it gives rise to a narrow resonance whose width is determined by the ground-state decay rate or transit time [1,20].

The experimental investigation of the response of atomic systems with quasidegenerate ground states driven by mutually coherent optical fields tuned to the same GSHL gives us an opportunity to check the theoretical predictions concerning the possibility of CPT for atomic systems with different level degeneracies. In addition, in the case of a superposition of two-level systems, the atomic response can be compared to two-level atom theory.

## II. EXPERIMENTAL SETUP

The response of rubidium vapor to the presence of two copropagating laser fields with variable frequency offset tuned to the  $D2$  line (780 nm) was examined. The relevant energy levels are shown in Fig. 2. Notice that the excited-state hyperfine splitting is smaller than the Doppler linewidth at room temperature:  $\Delta\nu_D \approx 530$  MHz. The  $5P_{3/2}$  natural width is  $\gamma_e = 6$  MHz.

To achieve the transit time limit of spectral resolution, the mutual coherence of the exciting laser fields is essential while the absolute laser linewidth is less important. The laser linewidth contribution to the spectral width can be estimated as  $\Delta_1 + \Delta_2 - 2\Delta_{12}$ . Here  $\Delta_1$  and  $\Delta_2$  are the spectral line-

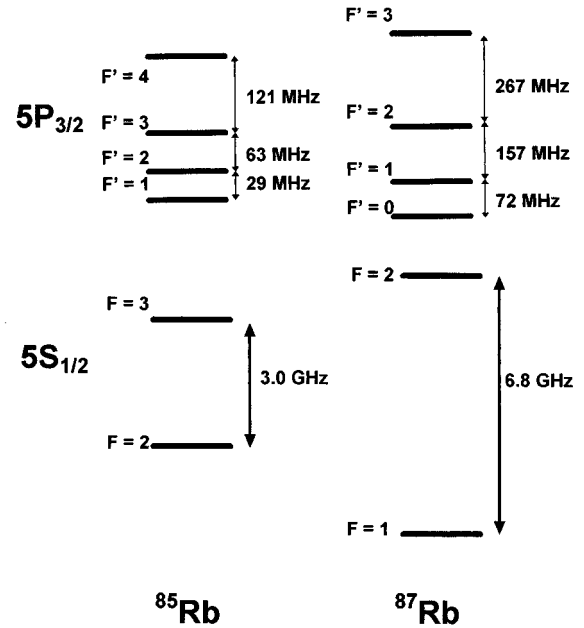


FIG. 2. Energy-level scheme for  $^{85}\text{Rb}$  and  $^{87}\text{Rb}$   $D2$  line.

widths of the laser waves, and  $\Delta_{12}$  is the cross-correlated width [3].

Several techniques can be explored to generate mutually coherent laser fields. The simplest is the laser frequency shifting by an acousto-optical modulator (AOM). If both GSHL's participate in the process, a GHz range frequency offset is needed for Rb, Cs, and Na that requires an elaborate setup [8,16]. However, since we concentrate on effects due to coherence involving magnetic sublevels within the same GSHL, a tunable optical frequency offset in the MHz range is sufficient. The required fields are easily generated with two consecutive AOM's.

The experimental scheme is shown in Fig. 3. The laser used was an extended cavity diode laser. The output power was typically 3 mW at 780 nm in a single mode regime. The laser linewidth was less than 1 MHz. To improve long term frequency stability the laser frequency was electronically locked to the transmission resonances of an external tunable 22-cm-long confocal Fabry-Pérot cavity (finesse  $\approx 30$ ). A small modulation at a frequency around 7 kHz is applied to the position of one of the mirrors of the Fabry-Pérot cavity. The transmitted signal is processed with a lock-in amplifier followed by a proportional and integrating amplifier to generate a correcting signal for laser frequency stabilization. With this system, the laser jitter remains below 1 MHz while the thermal drift is approximately 1 MHz/min (the typical spectrum acquisition time is less than 1 min). The two mutually coherent laser beams were produced by two AOM's. The undeflected output (zeroth order beam) of the first AOM (driven at a fixed frequency  $f_1 = 200.06$  MHz) was used as the pump beam. The +1 diffracted order of the first AOM was sent to a second AOM (driven at a tunable frequency  $f_2$ ) whose -1 diffracted order was used as the probe beam. We controlled the frequency offset  $\delta\nu = f_2 - f_1$  between the pump and probe beams by driving the second AOM with the help of a signal generator (Hewlett Packard 8647A). The value of  $f_2$  was varied from 185 to 215 MHz without sig-

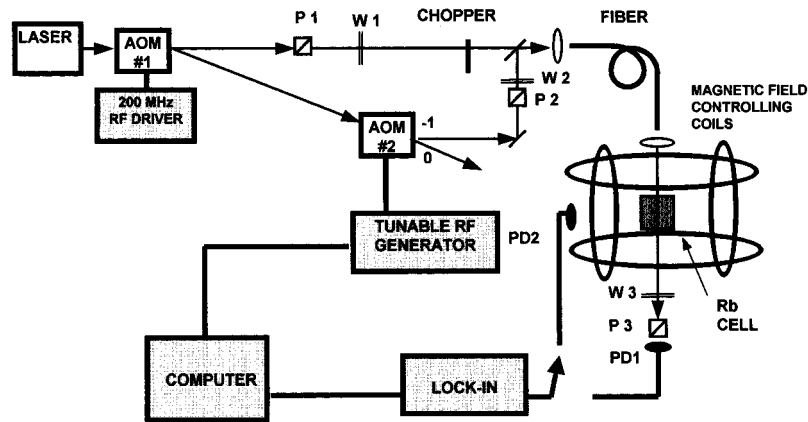


FIG. 3. Experimental setup. AOM, acousto-optic modulator;  $P1$ ,  $P2$ ,  $P3$ , polarizers;  $W1$ ,  $W2$ ,  $W3$ , waveplates;  $PD1$ ,  $PD2$ , photodiodes.

nificant reduction of the second AOM efficiency. The spectral width of the beat note between the pump and probe waves measured with a RF spectrum analyzer was smaller than the instrument resolution of 1 kHz.

A 3-cm-long glass cell containing a mixture of approximately equal amounts of the two Rb isotopes without buffer gas was used. The cell was kept at a temperature close to ambient in order to have a linear absorption of resonant radiation at the Rb  $D2$  lines of approximately 50%. The cell was placed within Helmholtz coils to control the strength and direction of the magnetic field at the sample. The magnetic field could be varied from zero to 2 G in an arbitrary direction. This is sufficient to remove the degeneracy of the ground-state Zeeman sublevels. However, the energy splitting remains below the natural width.

The polarizations of the pump and probe beams were independently set with the use of polarizers and  $\lambda/2$  or  $\lambda/4$  waveplates. The pump and probe waves were carefully combined with a dielectric beamsplitter into a bichromatic beam. No significant modification of the optical fields polarizations was introduced by the beam splitter or the glass cell. Alternatively, a polarizing cube beamsplitter was used. In this case, the combined optical fields have orthogonal linear polarizations. Using the unmodified combined beam or placing a linear polarizer or a quarterwave plate after the polarizing beamsplitter allows us to switch between linear and orthogonal, linear and parallel, or circular and opposite polarizations, respectively. Similar results were obtained with the two field combining schemes. The total available laser power at the cell was typically  $200 \mu\text{W}$  with a pump to probe intensity ratio of approximately 10. When a good optical quality and perfect overlap of the two fields was required, the combined beams were sent along a low-birefringence 50-cm-long single-mode optical fiber placed before the cell. The cross sections and intensities of the beams at the atomic sample were varied with the use of diaphragms, focusing lenses, and neutral density filters.

The light transmitted through the cell was focused into a  $5 \text{ mm}^2$   $p$ - $i$ - $n$  silicon photodiode ( $PD \#1$ ). When the transmission of only one beam was detected, a polarizer was placed between the cell and the photodiode to selectively detect the pump or the probe fields (linear orthogonal polarizations). The polarizer was preceded by a quarterwave plate for opposite pump and probe circular polarizations. The fluo-

rescence emitted by the atoms was monitored by a large-area ( $1 \text{ cm}^2$ ) silicon photodiode ( $PD \#2$ ). To eliminate the background due to linear absorption and to enhance the detection sensitivity we have used a lock-in amplifier together with a mechanical chopper (1 kHz) to process the signals from the photodiodes. The beam chopped was the pump (probe) when absorption (fluorescence) was monitored. A personal computer controlled the frequency offset  $\delta\nu = f_2 - f_1$  between the two beams and recorded the output of the lock-in amplifier.

### III. RESULTS

Figure 4 shows the total fluorescence emitted by the vapor as a function of the probe frequency offset in the case of the resonant transitions arising, respectively, from the two GSHL's  $F=2$  and 3 of  $^{85}\text{Rb}$ . There are several features visible on these broad-scanning-range spectra: (a) a slow variation of the baseline corresponding to the slope of the Doppler profile; (b) a Doppler-free resonance with homogeneous width  $\gamma_e$ ; (c) A subnatural-width peak or dip situated

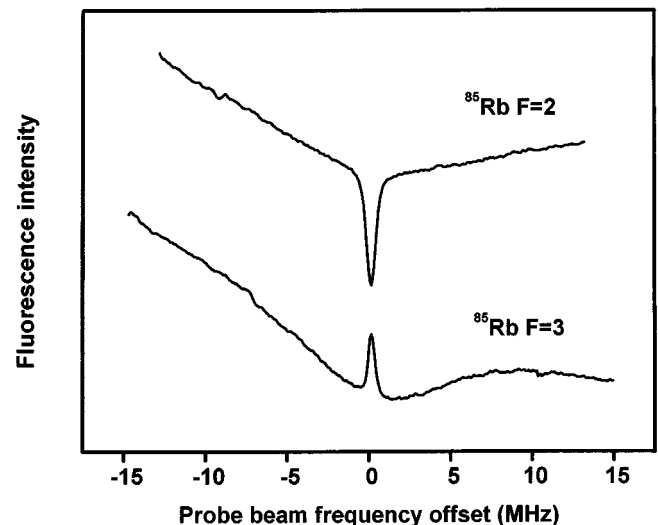


FIG. 4. Total atomic fluorescence as a function of the frequency offset between the pump and probe waves for the ground-state hyperfine levels  $F=2$  and 3 of  $^{85}\text{Rb}$ .

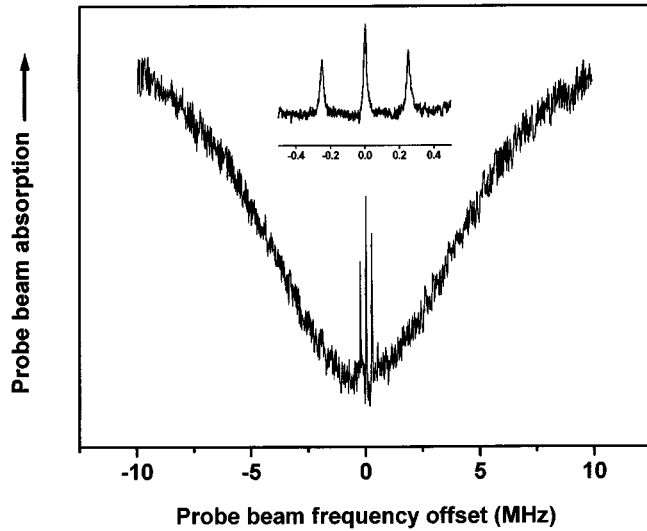


FIG. 5. Absorption of the pump beam as a function of the frequency offset between the two exciting laser fields for the ground-state hyperfine level  $F=3$  of  $^{85}\text{Rb}$ . The polarizations of the two beams are linear and orthogonal. A moderate magnetic field is applied along the lasers propagation axis.

on top of the Doppler-free resonance. Notice that this feature corresponds to a decrease of the fluorescence for the hyperfine level  $F=2$  and to an increase of the fluorescence in the case of level  $F=3$ . Analogous narrow resonances with opposite polarities were observed for GSHL's  $F=1$  and 2 of  $^{87}\text{Rb}$ .

Under the same conditions we have recorded the total transmission (of both beams) across the atomic cell. The observed results also present SNWR that correspond to increased absorption for level  $F=3$  and increased transparency for level  $F=2$  of  $^{85}\text{Rb}$ . If the absorption of only one beam (pump or probe) is detected, SNWR are also observed. Figure 5 shows the spectrum of the probe beam absorption for

GSHL  $F=3$  of  $^{85}\text{Rb}$  recorded in the presence of a magnetic field.

It must be emphasized that the observed SNWR cannot be explained only as an energy redistribution between the two laser fields. Although such a redistribution cannot be excluded, the fact that the resonances are present on the total absorption of the two beams and on the total atomic fluorescence clearly indicates a modification of the dissipative properties of the coherently driven atomic sample.

The amplitude of the observed SNWR depends on the laser polarizations. In general, the signal is larger for orthogonal polarizations than for the same polarizations. The SNWR amplitude can be comparable to or even larger than the amplitude of the Doppler-free resonance. We have observed SNWR corresponding to 20% variations with respect to linear absorption or fluorescence. In the following, we will concentrate on the spectral characteristics of the SNWR.

#### A. Magnetic-field dependence and selection rules

The external magnetic field breaks the hyperfine level degeneracy introducing a Zeeman splitting (see Fig. 5) given by

$$\Delta = (\mu_B / \hbar) g_F B, \quad (1)$$

where  $g_F = g_J [F(F+1) + J(J+1) - I(I+1)] / [2F(F+1)]$  is the composite Landé factor. Consequently, under the presence of a magnetic field the observed SNWR split into several components. We have analyzed the number and positions of the observed peaks for different combinations of the beam polarizations and magnetic-field orientation. The experimental results are summarized in Table I. All observations are consistent with electric dipole selection rules for Raman transitions between Zeeman sublevels of the ground-state involving one photon from the pump beam and another photon from the probe beam. Depending on the polarizations of the fields involved, the initial and final ground-state Zee-

TABLE I. Observed structure of the subnatural resonances for weak magnetic field for different combinations of the exciting field polarizations and magnetic field orientation. (The optical fields propagate along the  $z$  axis.)

Magnetic field orientation	Pump beam polarization	Probe beam polarization	Number of		
			observed peaks	Unshifted peak	Separation between adjacent peaks <sup>a</sup>
$z$	$x(y)$	$y(x)$	3	yes	$2\Delta$
$x$	$x$	$y$	2	no	$2\Delta$
$x$	$y$	$x$	2	no	$2\Delta$
$z$	$\sigma^+$	$\sigma^-$	1	no	$2\Delta^b$
$x$	$\sigma^+$	$\sigma^-$	5	yes	$\Delta$
$z$	$x$	$x$	3 <sup>c</sup>	yes	$2\Delta$
$x$	$x$	$x$	1 <sup>c</sup>	yes	0
$x$	$y$	$y$	3 <sup>c</sup>	yes	$2\Delta$
$z$	$\sigma^+$	$\sigma^+$	1 <sup>c</sup>	yes	0
$x$	$\sigma^+$	$\sigma^+$	5 <sup>c</sup>	yes	$\Delta$
oblique in $xz$ plane	$x$	$y$	5	yes	$\Delta$

<sup>a</sup>For fixed magnetic-field module.

<sup>b</sup>Peak position relative to zero probe-frequency offset.

<sup>c</sup>For lower ground-state hyperfine level only (see text).

man sublevels could differ in  $0$ ,  $\Delta$ , or  $2\Delta$ . As a check, the energy separation between peaks was measured as a function of the magnetic-field strength. The observed energy separation between adjacent Zeeman sublevels was measured to be  $0.47$  and  $0.71$  MHz/G for the ground-state levels of  $^{85}\text{Rb}$  and  $^{87}\text{Rb}$ , respectively, in good agreement with the values calculated from Eq. (1) and previous measurements [21].

It is interesting to note that for some particular polarizations, for instance  $\sigma^+$  pump and  $\sigma^-$  probe combination, a single narrow resonance is obtained. The position of this narrow feature relative to zero offset depends on magnetic field. This makes this resonance very attractive for CPT-based magnetometers [14]. Also, it is worth mentioning that we have observed SNWR corresponding to transitions from a given Zeeman sublevel to itself. In such a case, the position of the corresponding peak is not sensitive to the magnetic field. In the particular case of transitions arising from the upper GSHL ( $F=3$  for  $^{85}\text{Rb}$  and  $F=2$  for  $^{87}\text{Rb}$ ) we could not observe SNWR whenever the same polarization was used in the pump and the probe beam. Under similar conditions, the signal is clearly visible for the lower-lying GSHL on both isotopes.

### B. Line shape

We have concentrated on the magnetically insensitive peak. The shape of this peak depends on whether one field transmission, the total transmission, or the total fluorescence is monitored. In the case of fluorescence, the line shape closely approaches a Lorentzian function for all intensities used. When the transmission of only one of the two beams (pump or probe) is monitored, the line shapes visibly differ from a Lorentzian curve for intensities  $I > 1$  mW/cm $^2$ . For larger beam intensities the resonance becomes asymmetric approaching a dispersive curve.

### C. Linewidth

We have studied the dependence of the SNWR linewidth on different experimental factors. To avoid contributions from magnetic-field inhomogeneities, the measurements were carried on the magnetic-field-insensitive absorption peak with a magnetic field applied to the sample in order to have  $\Delta \gg \Gamma$ . The SNWR are very sensitive to the angle between the pump and probe beams. A 1 mrad misalignment is enough to clearly reduce the signal amplitude and introduce some broadening. To overcome this problem, both beams were sent through a single mode optical fiber to optimize overlap.

The influence of the time of flight across the light beam on the linewidth was investigated for small laser power. To do this, a variable diaphragm was placed before the cell to vary the diameter of the collimated combined optical beam. Before the diaphragm, the beam has a 1 cm diameter cross section and a divergence of less than 2 mrad. The results are presented on Fig. 6. The peak linewidth dependence on the inverse of the beam diameter is roughly linear with a coefficient of  $110 \pm 20$  kHz mm. This value is consistent with the estimated contribution to the linewidth of the atomic time of flight through the illuminated region. For larger beam diameter the linewidth approaches an asymptotic value around 6 kHz. The narrowest observed resonance has a full width at

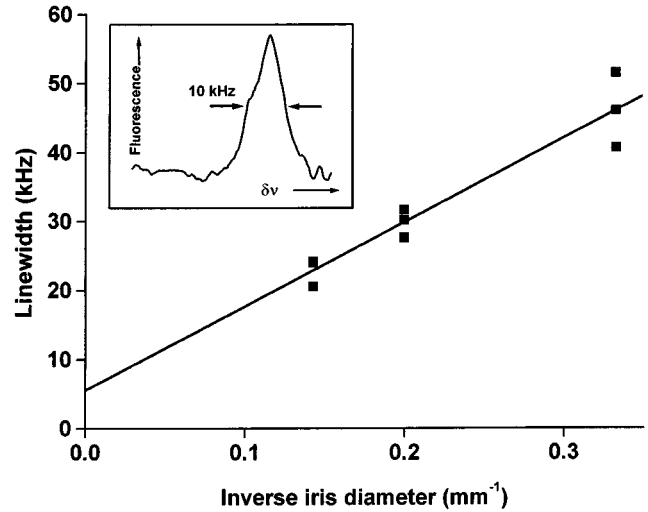


FIG. 6. Linewidth of the magnetically insensitive peak observed in the atomic fluorescence as a function of the inverse diameter of the exciting fields cross section. The inset shows the narrowest observed resonance.

half maximum of 10 kHz (Fig. 6).

The dependence of the width of the observed resonances on laser power was studied by varying the light intensity with the help of focusing lenses placed at variable distances from the sample and with neutral density filters placed on the overlapped beams while the alignment and polarizations of the beams remain constant. The observations are summarized in Fig. 7, where the estimated contributions from time of flight and angular misalignment were subtracted. At low intensities the laser power dependence of the linewidth is approximately linear with a coefficient of  $0.19 \pm 0.06$  MHz cm $^2$ /mW [3]. The deviation from linear dependence observed at high intensities may be due to laser beam inhomogeneity within the vapor cell.

## IV. DISCUSSION

It is well known that quantum interference can cancel the absorption of an atomic medium. An extensive survey of the theoretical work and the experimental evidence concerning the observation of this effect can be found in [3]. More re-

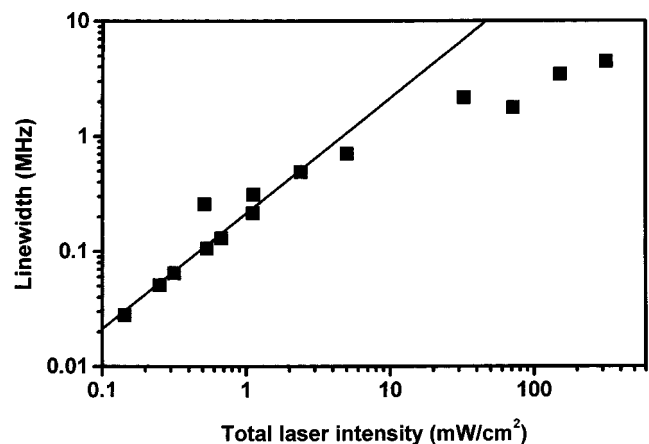


FIG. 7. Linewidth of the resonances observed in the atomic fluorescence as a function of the laser intensity in the excitation region. The pump and probe beams contribute with 90% and 10% of the laser intensity, respectively.

cently, EIT was observed in rubidium and cesium vapor using mutually coherent copropagating optical fields [22]. All these experiments demonstrate an increase in the atomic transparency due to the interaction with the optical fields. The results presented here constitute the first experimental evidence of the opposite effect: electromagnetically induced absorption.

A quantitative description of this phenomenon is presently at the stage of development. Nevertheless we can anticipate that it is related to the differences in structures of atomic level configurations involved in the interaction with radiation.

Let us consider in some detail the experimental situation. We have generally used two optical fields with a frequency offset  $\delta\nu < \gamma_e$ . In this case, due to the Doppler effect, the radiation excites atoms within three different velocity groups. For each velocity group, a different optical transition arising from the same GSHL is involved. Two of these transitions are so-called open transitions (radiative escape from the excited state to the nonresonant GSHL is possible). The third one is a cycling transition, for instance  $F=2 \rightarrow F'=1$  and  $F=3 \rightarrow F'=4$  for  $^{85}\text{Rb}$ . Since the time needed for the buildup of subnatural resonances is much longer than the excited-state lifetime  $1/2\pi\gamma_e$ , hyperfine optical pumping is very efficient [23]. As this causes the depletion of the initial state in the case of the two open transitions, we expect the main contribution to the SNWR to be due to the cycling transition.

For the lower GSHL of alkaline-metal atoms, the cycling transition takes place from a hyperfine level of total angular momentum  $F$  to an excited state of angular momentum  $F'=F-1$ . In such a case, SNWR that correspond to a decrease in the absorption and/or fluorescence were observed for any pump or probe polarization. On the other hand, no decrease in the absorption and/or fluorescence was obtained when the laser frequency was tuned to the upper GSHL, for which the cycling transitions takes place from a ground level of total angular momentum  $F$  to an excited state with  $F'=F+1$ . Instead, we observed for all but equal polarizations SNWR that correspond to an enhancement of the fluorescence and/or absorption with similar spectral properties to those corresponding to CPT. Our results confirm the validity of the theoretical predictions of [5] referred to the existence of CPT states. In addition, a new phenomenon is observed that indicates that when  $F' > F$  the atomic system is driven into a state with *constructive* quantum interference in the transition probability to the excited state. At present, the precise determination of the positively interfering state is not available. It will result from a careful examination of the atomic dynamics in the presence of the two driving fields explicitly taking into account the Zeeman structure of the atomic levels. Cal-

culations on these lines are currently underway.

A particular attention should be brought to the existence of a magnetically insensitive SNWR around zero frequency offset when the two optical waves have identical polarizations relative to the magnetic field orientation ( $\sigma^+$ ,  $\sigma^-$ , or  $\pi$ ). In this case, the fields address an ensemble of almost independent two-level systems only interconnected through spontaneous emission. According to Refs. [1] and [16] the coherent evolution of the two-level system gives rise to a narrow resonance in the probe transmission corresponding to an increased transparency. Consistently with this picture, we have observed a magnetically insensitive SNWR corresponding to increased transparency in the case of the lower GSHL using identical pump and probe polarizations. Under similar conditions, no narrow resonance (neither positive nor negative) was observed for the upper GSHL, suggesting that the increased transparency predicted by the two-level model is compensated by competing effects (presumably mediated by spontaneous emission).

## V. CONCLUSIONS

We have reported the observation of narrow spectral features associated to variations of the dissipative properties of an atomic medium in the presence of two resonant driving fields interacting with the same ground-state hyperfine level. In agreement with theoretical predictions, absorption dips due to CPT were observed for transitions with  $F \geq F'$  and not for  $F < F'$  for both Rb isotopes. However, for  $F > F'$  an unpredicted fluorescence and/or absorption peak was observed. This constitutes the first experimental evidence of electromagnetically induced absorption.

The observations reported here may have interesting applications for techniques relying on rapid variations of the absorption or the refractive index of an atomic medium. For instance, narrow absorption and/or dispersion resonances obtained on the same ground-state hyperfine level present some advantages for CPT-based magnetometers. On one hand, they offer the possibility to get a single magnetically dependent reference line. On the other hand, we have shown that resonances in the kHz range can be produced with a rather simple experimental setup. Finally, the resonance reversal reported here may lead to the observation of new effects such as steep dispersion with arbitrary polarity.

## ACKNOWLEDGMENTS

The authors wish to acknowledge technical assistance by A. Saez and H. Rodriguez. This work was supported by CONICYT (Uruguay) Project No. 92048 and the EU under Contract No. CII-CT93-0001.

---

[1] V. S. Letokhov and V. P. Chebotayev, *Nonlinear Laser Spectroscopy*, Springer Series in Optical Sciences Vol. 4 (Springer Verlag, Berlin, 1977).  
 [2] B. D. Agap'ev, M. B. Gornyi, B. G. Matisov, and Yu. V. Rozhdstvenskii, *Phys. Usp.* **36**, 763 (1993).

[3] E. Arimondo, Coherent Population Trapping [Prog. Opt. **XXXV**, 257 (1996)].  
 [4] H. R. Gray, R. M. Whyitley, and C. R. Stroud, *Opt. Lett.* **3**, 218 (1978).  
 [5] V. S. Smirnov, A. M. Tumaikin, and V. I. Yudin, *Zh. Eksp.*

- Teor. Fiz. **96**, 1613 (1989) [Sov. Phys. JETP **69**, 913 (1989)].
- [6] K.-J. Boller, A. Imamoglu, and S. E. Harris, Phys. Rev. Lett. **66**, 2593 (1991); J. E. Field, K. H. Hann, and S. E. Harris, *ibid.* **67**, 3062 (1991).
- [7] Yong-Quig Li and Min Xiao, Phys. Rev. A **51**, R2703 (1995).
- [8] A. S. Zibrov, M. D. Lukin, L. Hollberg, D. E. Nikonov, M. O. Scully, H. G. Robinson, and V. L. Velichansky, Phys. Rev. Lett. **76**, 3935 (1996).
- [9] A. S. Zibrov, M. D. Lukin, D. E. Nikonov, L. Hollberg, M. O. Scully, V. L. Velichansky, and H. G. Robinson, Phys. Rev. Lett. **75**, 1499 (1995).
- [10] S. E. Harris, J. E. Field, and A. Imamoglu, Phys. Rev. A **64**, 1107 (1990).
- [11] M. Kasevich, D. S. Weiss, E. Riis, K. Moler, S. Kasapi, and S. Chu, Phys. Rev. Lett. **66**, 2297 (1991).
- [12] S-Q. Shang, B. Sheehy, H. Metcalf, P. van der Straten, and G. Nienhuis, Phys. Rev. Lett. **67**, 1094 (1991).
- [13] A. M. Akulshin and M. Ohtsu, Quantum Electron. **24**, 561 (1994).
- [14] M. O. Scully and M. Freischhauer, Phys. Rev. Lett. **69**, 1360 (1992); S. Brandt, A. Nager, O. Schmidt, R. Wynands, and D. Meschede, in *1996 Conference on Precision Electromagnetic Measurements, Digest*, edited by A. Braun (IEEE, Piscataway, NJ, 1996), p. 190.
- [15] A. Kasapi, Phys. Rev. Lett. **77**, 1035 (1996).
- [16] O. Schmidt, R. Wynands, and D. Meschede, Phys. Rev. A **53**, R27 (1996).
- [17] D. Grison, B. Lounis, C. Salomon, J. Y. Courtois, and G. Grynberg, Europhys. Lett. **15**, 149 (1991).
- [18] J. W. R. Tabosa, G. Chen, Z. Hu, R. B. Lee, and H. J. Kimble, Phys. Rev. Lett. **66**, 3245 (1991).
- [19] T. van der Veldt, J. F. Roch, P. Grelu, and P. Grangier, Opt. Commun. **137**, 420 (1996).
- [20] E. V. Baklanov and V. P. Chebotaev, Zh. Eksp. Teor. Fiz. **61**, 922 (1971) [Sov. Phys. JETP **34**, 490 (1972)]; S. Haroche and F. Hartmann, Phys. Rev. A **6**, 1280 (1972).
- [21] H. G. Robinson and C. E. Johnson, Appl. Phys. Lett. **40**, 771 (1982).
- [22] J. Gea-Banacloche, Yong-qing Li, Shao-zhen Jin, and Min Xiao, Phys. Rev. A **51**, 576 (1995); Yong-qing Li and Min Xiao, *ibid.* **51**, R2703 (1995); D. J. Fulton, S. Shepard, R. R. Moseley, B. D. Sinclair, and M. H. Dunn, *ibid.* **52**, 2302 (1995); O. Schmidt, R. Wynands, Z. Hussein, and D. Meschede, *ibid.* **53**, R27 (1996).
- [23] The light intensity requirements for the observation of CPT and for saturation absorption due to hyperfine optical pumping in alkaline atoms are the same (see Refs. [2] and [3]).